

INFLUENCE OF THE CRACK TIP MODEL ON RESULTS OF THE FINITE ELEMENTS METHOD

MARCIN GRABA
JAROSŁAW GAŁKIEWICZ

*Faculty of Mechatronics and Machine Design, Kielce University of Technology
e-mail: mgraba@eden.tu.kielce.pl; jgalka@eden.tu.kielce.pl*

The paper contains recommendations of finite element models of the crack tip neighborhood to obtain results independent of the finite element mesh. The recommendations are valid for elastic-plastic problems and finite strains. As an example, analysis of single edge notched specimens under bending is presented.

Key words: fracture mechanics, finite deformation, stress distribution, J -integral, CTOD, finite elements method

1. Introduction

The Finite Elements Method (FEM) requires proper modeling of a given problem. The modeling concerns specimen geometry, description of a material, selection of the proper Finite Elements (FE) mesh.

The Hutchinson, Rice and Rosengren (HRR) solution (Hutchinson, 1968; Rice and Rosengren, 1968) of stress, strain and displacement fields near the crack tip for non-linear (elastic-plastic) materials concerns small strains and consists of one singular term only.

The amplitude of the singular stress field is the J -integral. The J -integral is path independent when the strain energy is a unique function of strains.

However, the stress distribution for a plane strain model is in most cases different from the HRR solution (see Fig. 1). This difference between the FEM stress distribution and the HRR solution was called by O'Dowd and Shih the " Q -parameter" (O'Dowd and Shih, 1991, 1992). In fact, the $Q\sigma_0$ term (where σ_0 is yield stress), when added to the HRR singular term, replaces all neglected terms in the asymptotic expansions of the stress field in front of the crack.

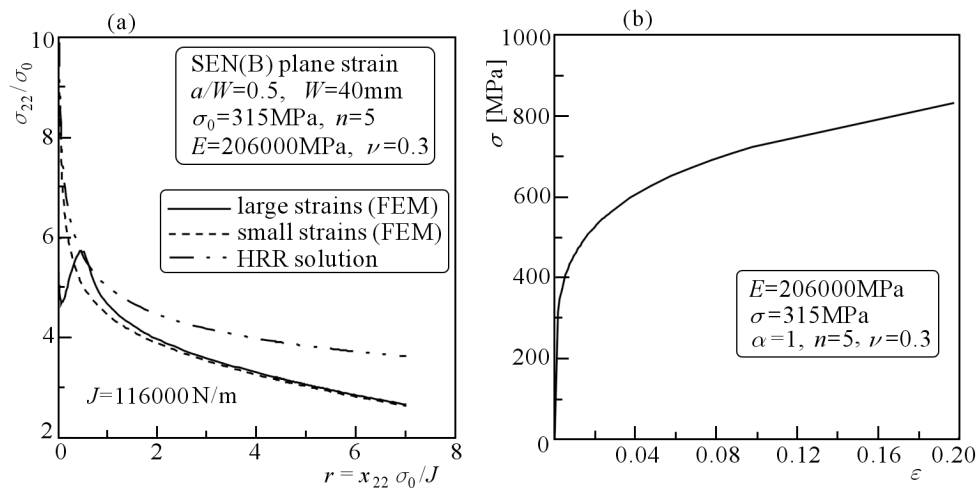


Fig. 1. (a) The stress distribution near the crack tip. Curves obtained using FEM for small and finite strain and HRR formula; (b) the stress-strain curve of the material used in FEM analysis

In a real structural element with a crack, stresses near the crack tip are finite. The stress infinity is a result of the assumption that the crack tip is perfectly sharp and it remains sharp during loading of the crack tip. When the assumption of small strains is relaxed, the crack tip blunts and the stresses in front of the crack become finite. The opening stress reaches maximum at the distance equal to $r = 0.5J/\sigma_0$ to $r = 2J/\sigma_0$, and its value depends on material properties, specimen geometry and external loading. This feature was first noticed by Rice and Johnson (1970), McMeeking and Parks (1979).

FE analysis of the stress and strain field in front of the crack when the finite strains are used is not a trivial problem. The level of the stress maximum and its localization depends on FE mesh details when it is not properly selected. For the small strain option, such a problem is not observed (ODowd and Shih, 1992; Al-Ani and Hancock, 1991; O'Dowd, 1995; O'Dowd *et al.*, 1995).

2. Numerical model

Numerical results are presented for single edge notched bend specimens (SEN(B)). Dimensions of the specimens satisfy requirements of the ASTM E 1820-05 standard. Computations were performed for a plane strain using the finite strain option. The relative crack length was $a/W = 0.5$, where a is the crack length, and the width of specimens W was equal to 40 mm.

The computations were performed using ADINA SYSTEM 8.3. Due to the symmetry, only a half of the specimen was modeled. The finite element mesh was filled with 9-node plane strain elements. The size of finite elements in the radial direction was decreasing towards the crack tip, while in the angular direction the size of each element was kept constant. It varied from $\Delta\theta = \pi/13$ to $\Delta\theta = \pi/23$ for various cases tested. The crack tip region was modeled using 6, 16, 35 and 75 semicircles. The crack tip was modeled as an arc whose radius varied from 0.0001 mm to 0.01 mm, $(10^{-6}(W - a))$ to $10^{-4}(W - a)$, respectively).

The Poisson ratio which was $\nu = 0.3$, the yield stress $\sigma_0 = 315$ MPa, Young's modulus $E = 206000$ MPa and the work hardening exponent $n = 5$ defined mechanical properties of the material. The true stress-strain curve used in FEM analysis is presented in Fig. 1b. In the model, the stress-strain curve was approximated by relation

$$\frac{\varepsilon}{\varepsilon_0} = \begin{cases} \frac{\sigma}{\sigma_0} & \text{for } \sigma \leq \sigma_0 \\ \alpha \left(\frac{\sigma}{\sigma_0}\right)^n & \text{for } \sigma > \sigma_0 \end{cases} \quad (2.1)$$

where ε_0 denotes the reference strain ($\varepsilon_0 = \sigma_0/E$) and α is a hardening constant, which was assumed 1 in this case.

3. Results of finite elements analysis

The numerical analysis of the stress distribution in the domain next to the crack tip revealed that results depend on the details of FE modeling, when the finite strain option is adopted. It is shown in Fig. 2 and Fig. 3. One may notice that when the number of the FEs between the crack tip and the maximum location of the opening stress is not large enough for the results to converge to a single curve. It is recommended to use at least 20 FEs between the crack tip and the stress maximum location. Thus, the FE size in the radial direction should be smaller than $0.1\delta_T$, where δ_T is the Crack Tip Opening Displacement (CTOD).

In contrast to the FE size in the radial direction, the size in the angular direction does not effect the stress distribution in front of the crack at $\theta = 0^\circ$. Several cases for the FE modeled as semicircular rings were tested (from 13 to 23 segments). The results are shown in Fig. 4.

In the literature, the crack tip is modeled in two different ways shown in Fig. 5c and Fig. 5d.

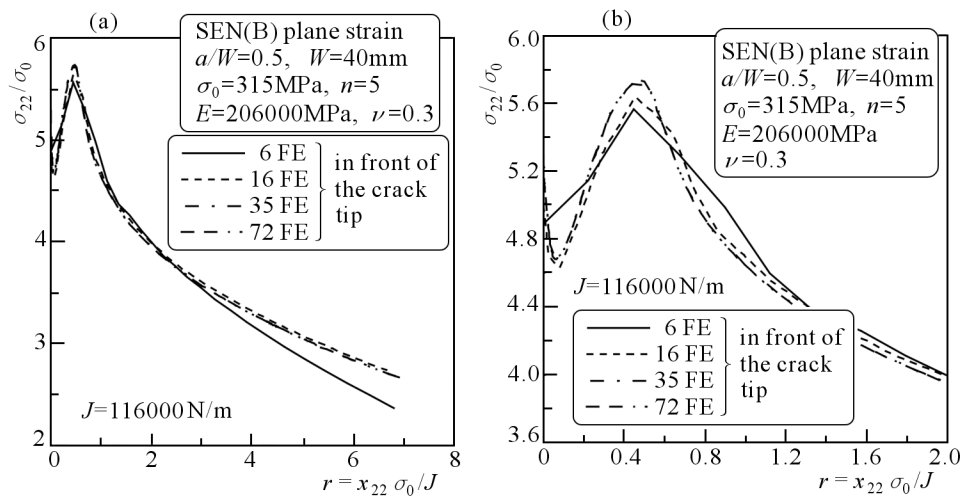


Fig. 2. Influence of the number of FE between the crack tip and the maximum location of the opening stress σ_{22} along the $\theta = 0^\circ$ direction on the stress distribution: (a) $r \leq 6J/\sigma_0$; (b) $r \leq 2J/\sigma_0$

Brocks *et al.* (2003) and Brocks and Scheider (2003) suggests that the crack tip should be modeled in the way shown in Fig. 5d. Computations confirm that when this model is used, the radius of the crack tip can be smaller than for the model shown in Fig. 5c to conduct the FE analysis for larger external loads.

O'Dowd and Shih (1991, 1992), O'Dowd (1995), O'Dowd *et al.* (1995) suggests that the crack tip radius should be smaller than the half of the crack tip opening displacement δ_{Tc} for the critical moment

$$r_w = \frac{1}{2}\delta_{Tc} = \frac{1}{2}d_n \frac{J_c}{\sigma_0} \quad (3.1)$$

where J_c is the critical value of the J -integral (for the material used in the FEM analysis: $J_c = 40 \text{ kN/m}$) and d_n is a parameter introduced by Shih, which connects the J -integral, yield stress and crack tip opening displacement (in our case $d_n = 0.297$). The crack tip radius calculated from equation (3.1) is equal to $r_w = 1.89 \cdot 10^{-5} \text{ m}$ and is greater than the crack tip radii tested in the FEM analysis which seemed to be advisable.

However O'Dowd was not interested in the opening stress distribution at the distance $r < J/\sigma_0$ which is of vital interest in our analysis. He used the small strain option during computation.

The FEM analysis shows that when the crack tip radius ρ decreases, the level of the maximum of the opening stress in front of the crack increases

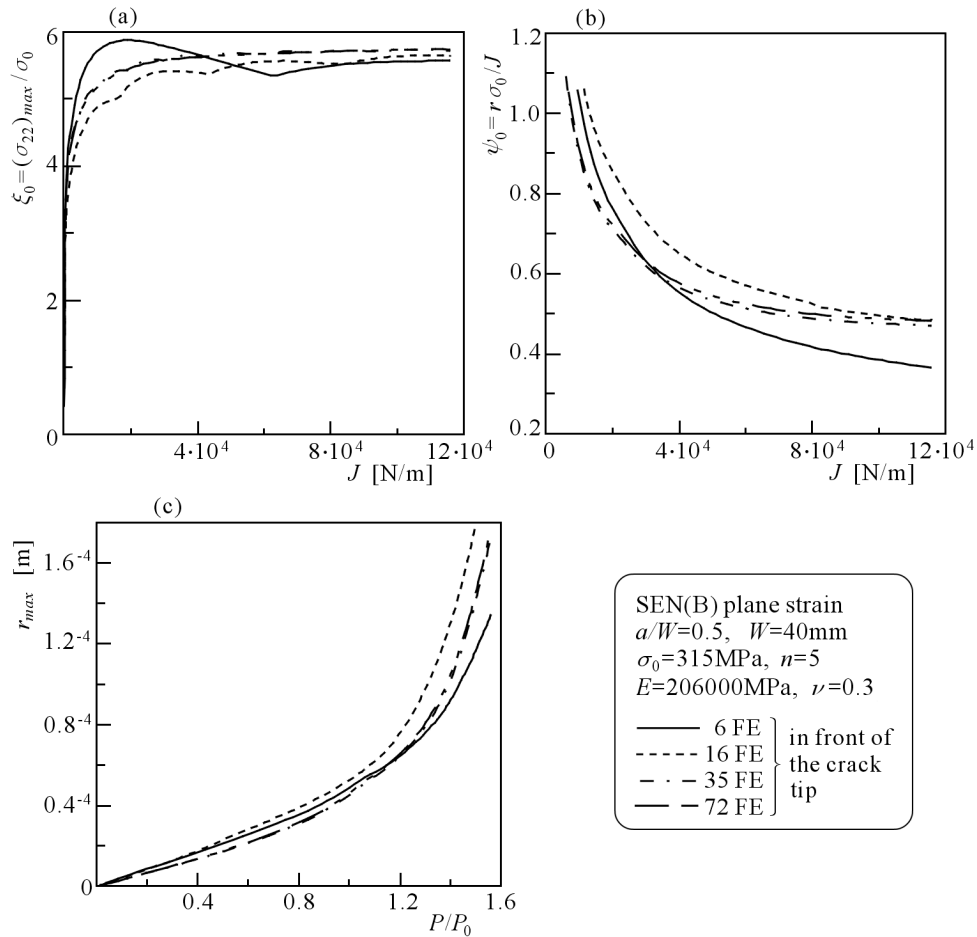


Fig. 3. Influence of the number of FE between the crack tip and the maximum location of the opening stress σ_{22} along the $\theta = 0^\circ$ direction: (a) the level of the maximum opening stress as a function of the external loading ($J_{IC} = 40000 \text{ N/m}$ for this material); (b) normalized location of the opening stress maximum as a function of the external load; (c) location of the opening stress maximum as a function of the external loading (P_0 is the limit load)

and appears closer to the crack tip. However, for a sufficiently small value of ρ , both the opening stress maximum and its location in front of the crack become independent of the crack tip radius. For increasing external load, the saturation of the $\xi_0 = \xi_0(J)$ and $\psi_0 = \psi_0(J)$ (where $\xi_0 = (\sigma_{22})_{max} / \sigma_0$ and $\psi_0 = (r_{22})_{max} \sigma_0 / J$) curves was observed (see Fig. 6). The curves level off, and the level is independent of the crack tip radius. Convergence of the FEM results is observed, when ρ is about $2.5 \cdot 10^{-6} \text{ m}$ ($\delta_{Tc}/15$ for the critical moment when the J -integral value is equal to $J_c = 40 \text{ kN/m}$, respectively).

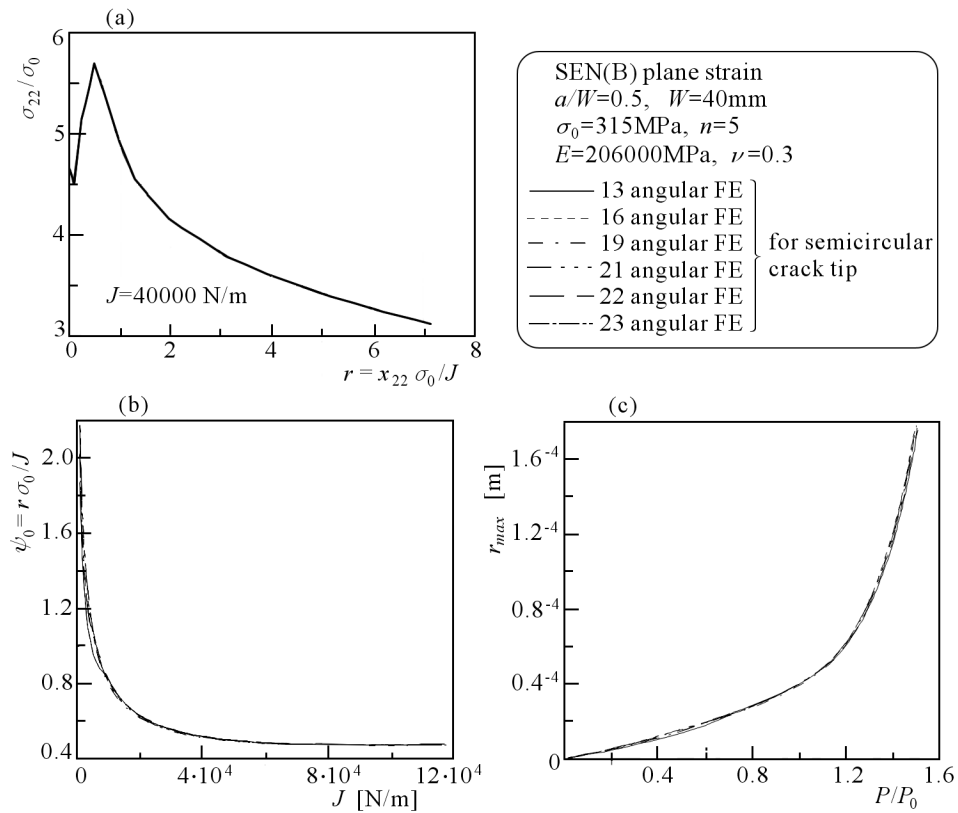


Fig. 4. Influence of the FE size in the tangential direction on FE results: (a) stress distributions in front of the crack tip for different levels of external loads (results for the $\theta = 0^\circ$ direction); (b) normalized distance of the maximum opening stress to the crack tip; (c) distance of the maximum opening stress to the crack tip

Thus the crack tip model shown in Fig. 5d is recommended.

4. Estimation of the J -integral

In this section, the influence of size of contour of integration on the J -integral is investigated. In ADINA SYSTEM 8.3, the J -integral may be calculated by making use of two methods.

The first method is based on the J -integral definition

$$J = \int_C \left(w dx_2 - \mathbf{t} \frac{\partial \mathbf{u}}{\partial x_1} \right) ds \quad (4.1)$$

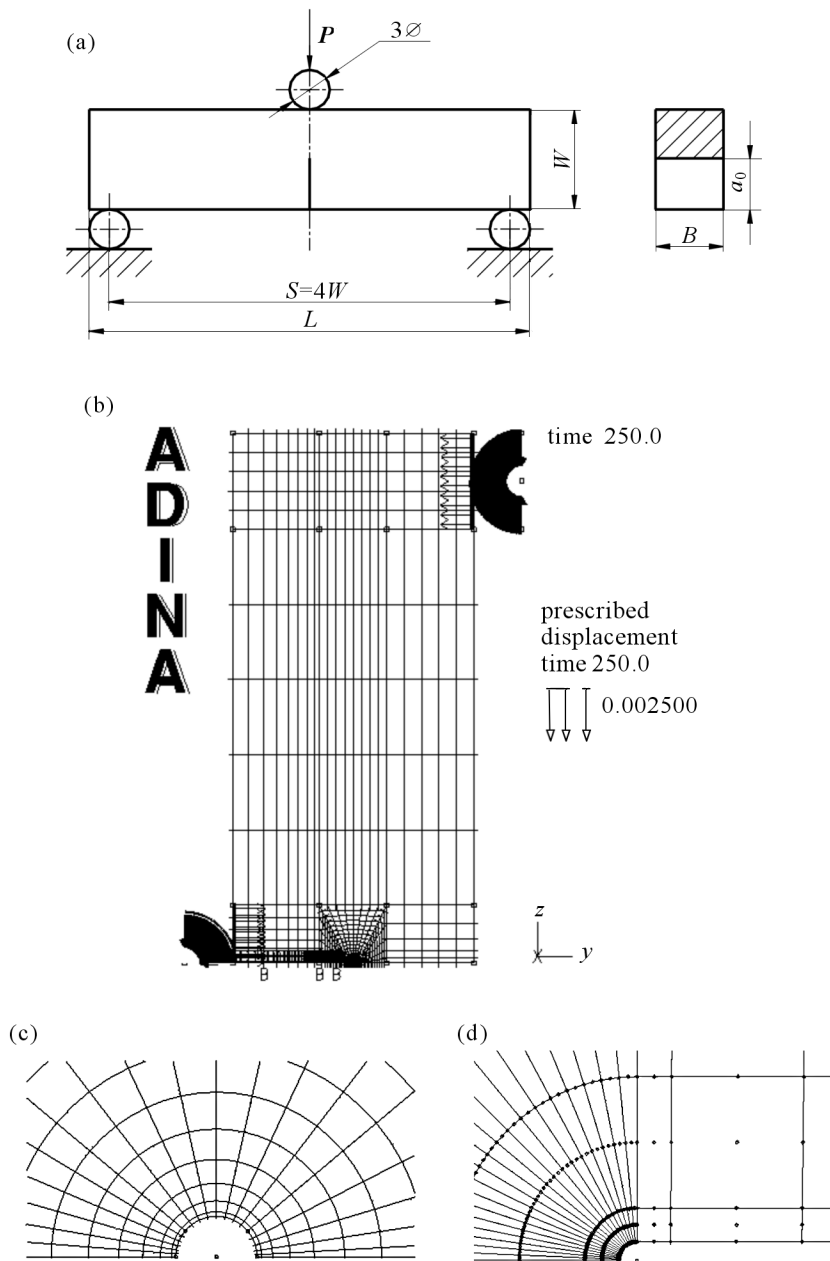


Fig. 5. (a) SEN(B) specimen; (b) FEM mesh for SEN(B) specimen; (c), (d) two alternative crack tip models

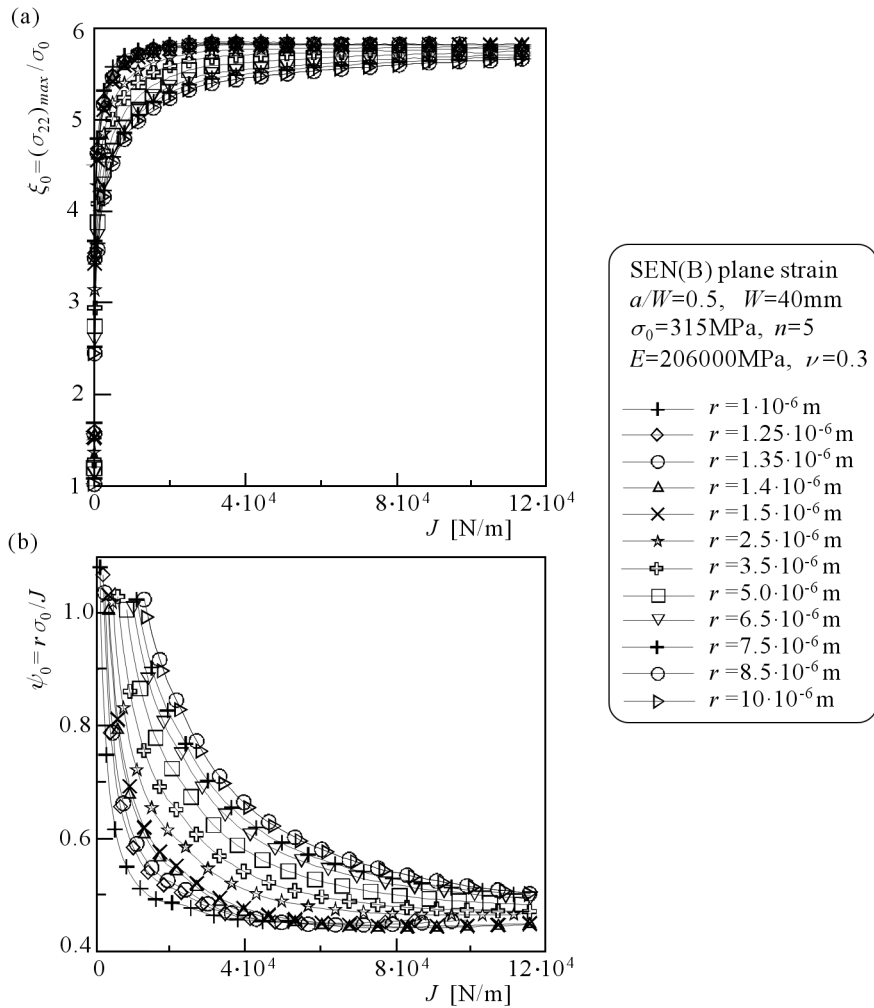


Fig. 6. Effect of size of the crack tip radius on: (a) level of the maximum opening stress; (b) normalized location of the maximum opening stress

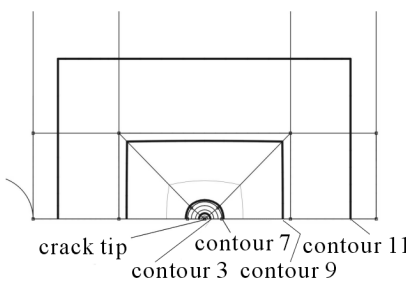
where w is the strain energy density, \mathbf{t} is the stress vector acting on the contour C drawn around the crack tip, \mathbf{u} denotes the displacement vector and ds is an infinitesimal segment of the contour C .

The second method, called the "virtual shift method", uses the concept of virtual crack growth to compute the virtual energy change.

The J -integral is path independent for small strain formulation only. However, one may also calculate the J -integral using the large strain formulation, but the contour of integration should be sufficiently distant from the crack tip and not too close to the specimen borders.

In Table 1, the contours of integration used in this investigation are shown.

Table 1. Definition of J -integral contours

	Number of contour	Distance form crack tip [mm]
	1	0.02
2	0.15	
3	0.36	
4	0.67	
5	1.08	
6	1.59	
7	2.25	
8	4.64	
9	9.39	
10	18.0	
11	18.0	

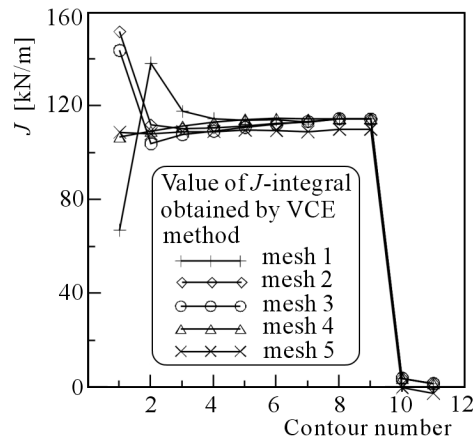


Fig. 7. Effect of size of the integral contour and the mesh size on the numerically found J -integral

Figure 7 presents J -integral values obtained for different contours and different meshes. The smallest FE mesh (the first mesh in Table 2) used in the analysis was extremely dense. Subsequent meshes were gradually sparse. Every mesh but the last (the fifth mesh in Table 2) were filled with 9-nodes elements. In the fifth mesh, 4-nodes finite elements were used.

The calculations confirm that the J -integral is almost independent of the finite elements used in FEM analysis. The most important is the way the contour of integration is drawn. It should not lie too close to the crack tip nor

to the edge of the specimen. The best recommendation is to use a few different integral contours in FEM analysis and compare the results.

Table 2. Definition of FE meshes used for calculation of the J -integral

Mesh	Number of elements between crack tip and maximum opening stress for critical moment $J_c = 40 \text{ kN/m}$	Nodes per element
mesh 1	72	9
mesh 2	35	9
mesh 3	16	9
mesh 4	6	9
mesh 5	36	4

5. Determination of the crack tip opening displacement

The Crack Tip Opening Displacement (CTOD) is determined using the method proposed by Shih (1981) (see Fig. 8). The most important problem here is the choice of the crack tip model. In our calculations, we used three models of the crack tip.

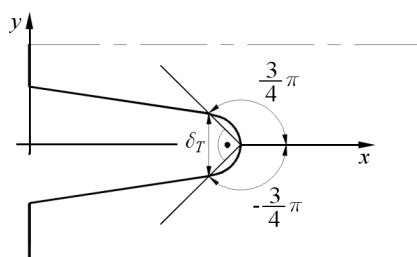


Fig. 8. Shih's method proposed for determination of the crack opening displacement

In the most common model called hereafter "sharp", the crack tip radius is equal to zero. In the second model, the crack tip is modeled as a half of the circle (see Fig. 5c) and in the last one, the crack tip is in a form of the quarter of the circle (see Fig. 5d). In the third model, the initial value of CTOD is equal to the radius of the crack tip circle.

The results obtained show (see Fig. 9) that the best results, which are close to the theoretical plane strain value of CTOD (Shih, 1981), are obtained for the sharp crack tip model, and the worst results – with a half of the circle. Unfortunately, two of the three models are unable to determine the CTOD for small external loads, which in Fig. 9 are represented by the J -integral level. To

determine the CTOD for the complete spectrum of external loads, we suggest to use the third model (see Fig. 5d).

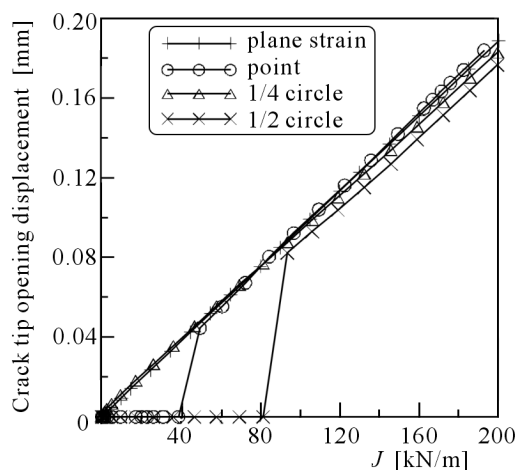


Fig. 9. Changes of the CTOD for growing external load

6. Conclusions

In the paper, the influence of finite element mesh size and the crack tip model on FEM results was discussed. In particular, the stress distribution in front of the crack for the finite strain option was analyzed. It is important that the size of elements in front of the blunted crack should be less than $0.1 \cdot \text{CTOD}$ for the critical moment.

The crack tip radius should be of the order of 10^{-6} - 10^{-7} m. The size of the crack tip radius is not important if the stresses are measured at the distance $r > J/\sigma_0$ and when it increases to the value three times greater than the initial one. We propose to use the crack tip model shown in Fig. 5d when the large strain formulation is used.

The calculations show that the J -integral can be determined using quite large finite elements if "the virtual shift method" is used. The contour of integration, which is used to determine the J -integral, must not lie too close to the crack tip and to the edge of the specimen. It should not cross the border between the plastic and elastic zone if it is possible.

To calculate the crack tip opening displacement, we suggest using the crack tip model shown in Fig. 5d. This model allows one to determine the CTOD value for the whole spectrum of external loads.

Acknowledgements

We are pleased to acknowledge helpful interactions and discussions with prof. A. Neimitz from Kielce University of Technology.

The work presented in this paper was conducted with support of Polish State Committee for Scientific Research, grant No. 5 T07C 004 25.

References

1. AL-ANI A.M., HANCOCK J.W., 1991, J -dominance of short cracks in tension and bending, *J. Mech. Phys. Solids*, **39**, 1, 22-43
2. BROCKS W., CORNEC A., SCHEIDER I., 2003, Computational aspects of nonlinear fracture mechanics, *Bruchmechanik, GKSS-Forschungszentrum, Geesthacht*, Germany, Elsevier, 127-209
3. BROCKS W., SCHEIDER I., 2003, Reliable J -values. Numerical aspects of the path-dependence of the J -integral in incremental plasticity, *Bruchmechanik, GKSS-Forschungszentrum, Geesthacht*, Germany, Elsevier, 127-209
4. GRABA M., GAŁKIEWICZ J., 2005, Wpływ modelu wierzchołka pęknięcia na wyniki uzyskane metodą elementów skończonych, *Materiały Konferencyjne X Konferencji Mechaniki Pękania*, 333-342, Opole, Wisła
5. HUTCHINSON J.W., 1968, Singular behaviour at the end of a tensile crack in a hardening material, *Journal of the Mechanics and Physics of Solids*, **16**, 13-31
6. McMEEKING R.M., PARKS D.M., 1979, On criteria for J -dominance of crack tip fields in large scale yielding, *ASTM STP 668, American Society for Testing and Materials*, Philadelphia, 175-194
7. O'DOWD N.P., 1995, Applications of two parameter approaches in elastic-plastic fracture mechanics, *Engineering Fracture Mechanics*, **52**, 3, 445-465
8. O'DOWD N.P., SHIH C.F., 1991, Family of crack-tip fields characterized by triaxiality parameter. I – Structure of fields, *Journal of Mechanics and Physics of Solids*, **39**, 8, 989-1015
9. O'DOWD N.P., SHIH C.F., 1992, Family of crack-tip fields characterized by triaxiality parameter. II – Fracture applications, *Journal of Mechanics and Physics of Solids*, **40**, 5, 939-963
10. O'DOWD N., SHIH C.F., DODDS R.H. JR., 1995, The role of geometry and crack growth on constraint and implications of ductile/brittle fracture, *ASTM STP 1244, American Society for Testing and Materials*, Philadelphia
11. RICE J.R., JOHNSON M.A., 1970, The role of large crack tip geometry changes in plane strain fracture, In: *Inelastic Behaviour of Solids*, M.F. Kanninen, McGraw-Hill, 641-672

12. RICE J.R., ROSENGREN G.F., 1968, Plane strain deformation near a crack tip in a power-law hardening material, *Journal of the Mechanics and Physics of Solids*, **16**, 1-12
13. SHIH C.F., 1981, Relation between the J -integral and the crack opening displacement for stationary and extending cracks, *Journal of Mechanics and Physics of Solids*, **29**, 305-329

Wpływ modelu wierzchołka pęknięcia na wyniki uzyskane metodą elementów skończonych

Streszczenie

W pracy przeprowadzono analizę wpływu modelu MES na wartość naprężeń przed frontem pęknięcia w materiałach sprężysto-plastycznych, wyznaczaną w sposób numeryczny wartość całki J oraz rozwarcie wierzchołka pęknięcia (RWP). Obliczenia prowadzono dla płaskiego stanu odkształcenia przy założeniu dużych odkształceń.

Manuscript received June 14, 2006; accepted for print February 21, 2007